

Novel synthesis approach for "stubborn" metals and metal oxides

William Nunn^a, Anusha Kamath Manjeshwar^a, Jin Yue^a, Anil Rajapitamahuni^a, Tristan K. Truttmann^a and Bharat Jalana,10

^aDepartment of Chemical Engineering and Materials Science, University of Minnesota, Twin Cities, Minneapolis, MN 55455

Edited by S. S. P. Parkin, Max Planck Institute of Microstructure Physics, Halle (Saale), Germany, and approved June 28, 2021 (received for review March

Advances in physical vapor deposition techniques have led to a myriad of quantum materials and technological breakthroughs, affecting all areas of nanoscience and nanotechnology which rely on the innovation in synthesis. Despite this, one area that remains challenging is the synthesis of atomically precise complex metal oxide thin films and heterostructures containing "stubborn" elements that are not only nontrivial to evaporate/sublimate but also hard to oxidize. Here, we report a simple yet atomically controlled synthesis approach that bridges this gap. Using platinum and ruthenium as examples, we show that both the low vapor pressure and the difficulty in oxidizing a "stubborn" element can be addressed by using a solid metal-organic compound with significantly higher vapor pressure and with the added benefits of being in a preoxidized state along with excellent thermal and air stability. We demonstrate the synthesis of high-quality single crystalline, epitaxial Pt, and RuO2 films, resulting in a record high residual resistivity ratio (=27) in Pt films and low residual resistivity, \sim 6 $\mu\Omega$ ·cm, in RuO₂ films. We further demonstrate, using SrRuO₃ as an example, the viability of this approach for more complex materials with the same ease and control that has been largely responsible for the success of the molecular beam epitaxy of III-V semiconductors. Our approach is a major step forward in the synthesis science of "stubborn" materials, which have been of significant interest to the materials science and the condensed matter physics community.

molecular beam epitaxy | synthesis | atomic layer control | evaporation | physical vapor deposition

mprovements in thin film deposition processes have broadly impacted many technology innovations and breakthroughs (1, 2), not only by shaping the current electronics industry but by also extensively affecting areas such as optics, solar cells, coatings, biomedical devices, and aerospace engineering. Developing synthesis techniques for material improvement is driven in part by the desire to achieve intrinsic properties in thin films, a challenge that has and continues to motivate materials scientists and physicists. However, as deposition processes have advanced, many new phenomena have been discovered due to the increased control over chemistry, structure, and defects. For example, it was the ability to grow a heterostructure with an interface very low in defects that led to the discovery of the integer and fractional quantum Hall effects (1985 and 1998 Physics Nobel Prize) (1). Similarly, new exotic phases such as two-dimensional electron gases and superconductivity have been made possible as a result of being able to grow heterostructures with these high-quality interfaces (3-5). Control over structure and defects has also led to ever-improving properties such as electron mobilities (6), in some cases, surpassing those of the bulk material itself (7). Finally, the additional advantage of epitaxial strain has allowed for an enhancement or emergence of certain material properties [e.g., ferroelectricity (8, 9) and superconductivity (10, 11)].

Common thin film synthesis approaches include the physical vapor deposition (PVD) techniques such as evaporation, sputtering, and pulsed laser deposition (PLD). Sputtering and PLD have advantages of high growth rates, compatibility with background gases, such as oxygen, and the ability to grow complex materials from a large variety of sputtered or ablated targets. However, due to the high kinetic energy involved in these processes, point defects can become a problem and potentially degrade material properties. Stoichiometry control can also be difficult, as the assumption that the stoichiometry of the target will transfer to the film is not always correct (12). Under the category of evaporation approaches, molecular beam epitaxy (MBE), on the other hand, is an ultra-high vacuum, low-energy PVD technique that excels not only at limiting these undesirable defects but also by giving unmatched control over stoichiometry, leading to record properties in numerous material systems (13). After its invention for the original purpose of atomically controlled synthesis of III-V semiconductors, MBE provided a route for the growth of high mobility modulation-doped structures (1) and also played a key role in developing a new class of high- T_c oxide superconductors that has advanced the way we think about oxide materials (3). This technique continues to drive the development of modern microelectronics and has greatly impacted the fundamental study of quantum materials and how we approach material design (14). However, in MBE and other PVD approaches, synthesis progress recently has largely relied on process optimization and improvements in vacuum level (15). Many materials have still proven challenging to grow, especially when they contain metals with ultra-low vapor pressures, which therefore require extremely high temperatures to evaporate or sublime.

Significance

Atomically precise complex oxides containing "stubborn" elements, such as ruthenium, iridium, and platinum, hold tremendous promise as designer quantum materials for exploring novel electronic, magnetic, superconducting, and topological phases owing to their strong spin-orbit interaction. This study shows a method to synthesize such materials by eliminating the major synthesis bottleneck of low vapor pressure and difficulty in oxidation. This study serves as a "proof-of-concept" allowing us to 1) grow Pt, RuO2, and SrRuO3 thin films by supplying Pt and Ru precursors at 65 to 100 °C in a lowtemperature effusion cell, as opposed to the several thousand degrees Celsius needed using electron beam evaporators; 2) reveal bulk-like room-temperature resistivity; and 3) ultimately provide pathways to creating atomically precise quantum structures.

Author contributions: W.N., A.K.M., and B.J. designed research; W.N., A.K.M., J.Y., A.R., and T.K.T. performed research; W.N., A.K.M., J.Y., A.R., T.K.T., and B.J. analyzed data; B.J. conceived the idea with W.N.; and W.N., A.K.M., J.Y., and B.J. wrote the paper.

The authors declare no competing interest.

This article is a PNAS Direct Submission

Published under the PNAS license

¹To whom correspondence may be addressed. Email: bjalan@umn.edu.

This article contains supporting information online at https://www.pnas.org/lookup/suppl/ doi:10.1073/pnas.2105713118/-/DCSupplemental.

Published August 5, 2021.

Fig. 1A shows the vapor pressures of a few commonly used metals (16) as well as the typical vapor pressure range used in MBE growth, 10^{-5} to 10^{-2} Torr. While, for example, effusion cells are suitable for the sublimation of Sr and Ba, which are commonly used in various complex oxides, or for evaporation of Al and Ga, used in GaAs/AlGaAs heterostructures, their use for refractory and noble metals such as Pt, Ru, Ir, and W can prove difficult or even impossible. Although recent innovation and progress in thermal laser evaporation is promising (17), to overcome the problem of low vapor pressures, most have traditionally turned to electron beam (e-beam) evaporation. This technique is capable of heating a material to much higher temperatures than an effusion cell. Although this allows for sufficient vapor pressure, difficulties can arise with maintaining a constant flux due to the localized heating and due to potential safety issues. Synthesizing thin films of complex materials can therefore become problematic, as controlling the relative fluxes of the precursor materials is key to stoichiometry control. Feedback control can be used to maintain the flux, but this can be complicated and add to the already large cost and complexity of e-beam evaporators (18).

Other problems can occur in PVD when growth is complicated with the addition of gases, such as oxygen, for the synthesis of oxide materials. Many metals have problems with source oxidation or low oxidation potentials such as Ti and Sn, respectively. For MBE, a modification of the conventional technique, known as hybrid or metal-organic MBE (MOMBE), has successfully overcome some of these issues by using metal-organic precursors for a few of the metals in question. These techniques utilize volatile metal-organic compounds, containing the desired metal, injected into the vacuum system through an external gas inlet system. Although metal-organic precursors have been found to address the issues of low vapor pressures, oxidation of source materials, and low oxidation potentials for metals like Ti (19), Sn (20), and V (21), it has been nontrivial to find suitable precursors for other metals.

To this end, we have developed a technique for supplying metallic elements for the growth of metals or metal-containing materials in PVD processes, specifically targeting ultra-low vapor pressure elements. Metal-organic compounds can be designed to supply these elements, partially or completely oxidized to the desired oxidation state and with additional oxygens bonded to the metallic center by the choice of suitable ligands. Specifically, if this metal-organic compound is a solid and thermally stable, it can be sublimed in an effusion cell at a relatively low temperature. We show that it is possible to deliver the desired metal for growth of high-quality single crystalline films and without the risk of oxidizing elemental sources and components of the vacuum chamber. Although similar to hybrid MBE, which also uses

metal-organic precursors, this technique differs in an important way. In hybrid MBE, precursors are usually evaporated as a liquid with a large vapor pressure of \sim 10 Torr at operating temperature. To achieve this, the precursor must be placed in a bubbler outside the vacuum chamber. By using a precursor that is solid and has an intermediate vapor pressure, we can place the compound in a conventional low-temperature effusion cell directly in the vacuum chamber irrespective of the background pressure. This technique thus solves the problem of it being difficult to find metal-organic compounds for hybrid MBE, which requires high vapor pressures and consequently liquid compounds in all reports thus far. For this reason, we are referring to this technique as solid source MOMBE. This process also differs from some solid source metalorganic chemical vapor deposition techniques (22, 23) because, with the precursor placed directly in the vacuum system, no carrier gas is needed, so a large mean free path is retained for growth when the background pressure is low.

Results

As a demonstration of the potential of this synthesis technique for the growth of ultra-low vapor pressure metals and metalcontaining oxides, we chose to grow a variety of materials, including the simple metal Pt, binary oxide RuO₂, and complex oxide SrRuO₃, using the metal-organic precursors platinum(II) acetylacetonate, Pt(acac)₂, and ruthenium(III) acetylacetonate, Ru(acac)₃. Pt films have been useful as electrodes for dielectric materials due to the high work function, and recent interest has also included the study of the spin Hall effect, where films low in defects are desired (24). RuO2 has been studied for its low resistivity and high chemical and thermal stability for applications such as electrodes in supercapacitors (25), catalysts in reactions like the oxygen evolution reaction (26), and, recently, for the discovery of superconductivity when strained (10). Finally, SrRuO₃ has been a material of significant interest due to its itinerant ferromagnetism, presence of the anomalous Hall effect, and for its use as electrodes in oxide electronics (27). Our work opens up a method for tackling the highly rewarding problem of stabilizing challenging metals like these for further use and study of these exciting phenomena and applications.

The metal-organics Pt(acac)₂ and Ru(acac)₃ were identified as suitable precursors due to their vapor pressures falling in the desired range at low temperatures, about 10⁻³ Torr at 100 °C (28). In fact, we were able to grow films here with source temperatures of only 65 to 85 °C for Pt and 100 °C for RuO₂. Fig. 1B shows the vapor pressure of Pt(acac)₂ and Ru(acac)₃ compared with metallic elements Ba and Sr and volatile metal-organics vanadium(V) oxytriisopropoxide, titanium(IV) tetraisopropoxide,

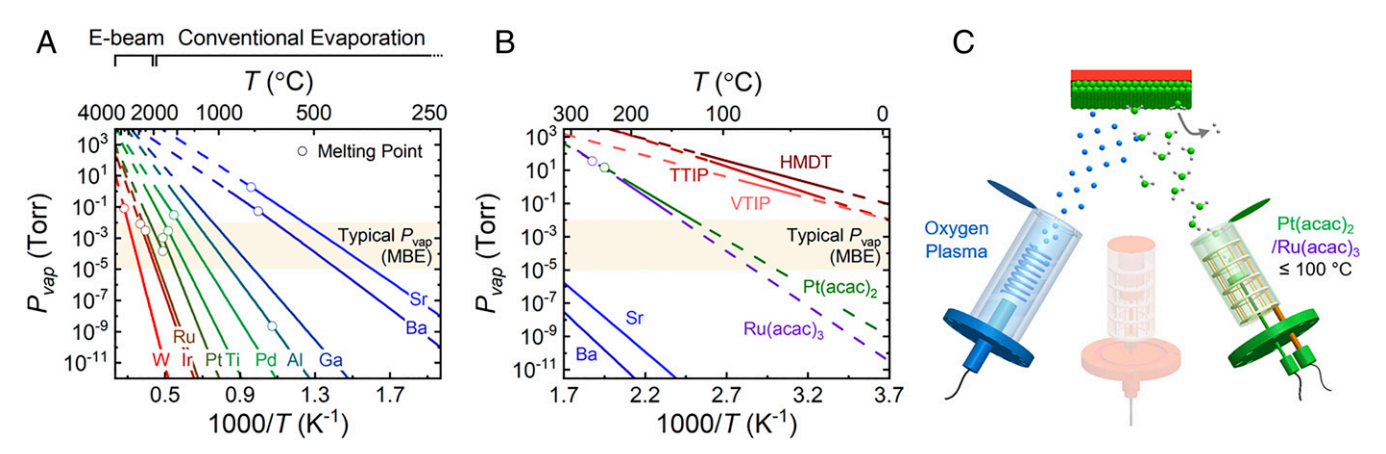


Fig. 1. (A) Vapor pressures (P_{vap}) for a variety of commonly used metals in thin film deposition processes. Dashed lines are linear extrapolations. (B) Vapor pressure of Pt(acac)₂ and Ru(acac)₃ compared with commonly used metal-organics and metals in MBE. (C) Schematic of solid source MOMBE technique.

Pt films were grown on SrTiO₃ (001) substrates using a Pt(acac)₂ source temperature of only 65 °C. The low-temperature sublimation led to films with structural characteristics very similar to previous reports of Pt films grown on SrTiO₃ (32-34). Phase-pure, epitaxial (001) oriented films were obtained for substrate temperatures ranging from 520 to 930 °C, shown in SI Appendix, Fig. S1, with the (111) orientation occurring at 400 °C. However, we did not find atomically smooth surfaces in these films. In fact, growing atomically smooth Pt films on dielectric substrates such as SrTiO₃ has historically been difficult due to the favorable agglomeration of metals on dielectric materials (35). Growing atomically smooth films, however, is desirable for heterostructure applications. Instead, here, we found that by changing to a conducting substrate, Nb-doped SrTiO₃, we were able to grow Pt films with these desired surfaces. We attribute it to the change in growth kinetics owing to an enhanced surface diffusivity of Pt adatoms on a conducting substrate. A 70-nm Pt film with a single peak in high-resolution X-ray diffraction (HRXRD) is shown in Fig. 24. Steps are seen on the surface from atomic force microscopy (AFM) images (Fig. 2B), with a step height of one Pt unit cell, showing this technique is able to grow films with an atomically smooth surface. Similar reflection high-energy electron diffraction (RHEED) patterns were obtained as those films grown at high substrate temperatures on undoped SrTiO₃ (SI Appendix, Fig. S1) but with more well-defined streaks, attesting to the high crystalline quality and smooth surface.

To test the electronic properties of the Pt films, a 70-nm film was grown at an intermediate SrTiO₃ substrate temperature of

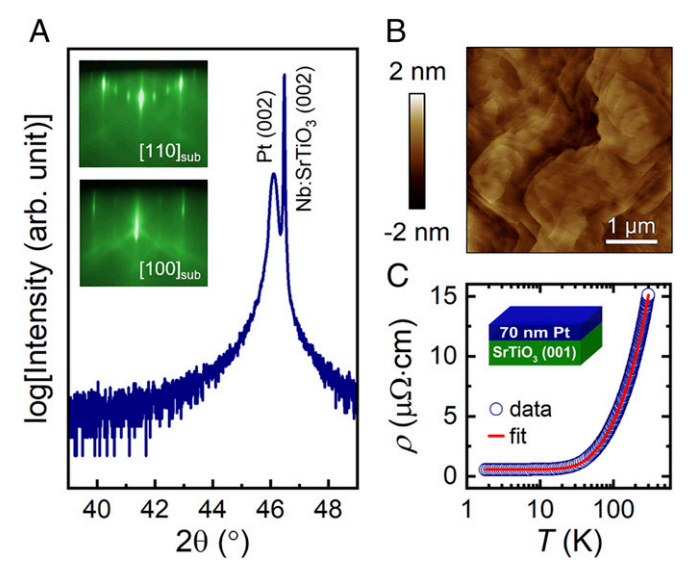


Fig. 2. (A) HRXRD and (B) AFM of 70-nm Pt film grown on conducting Nb-doped $SrTiO_3$ (001) substrate. Inset of A shows RHEED along the substrate [110] and [100] azimuths. (C) Resistivity of 70-nm Pt film grown on insulating $SrTiO_3$ (001) substrate. Red line is fit to Bloch–Grüneisen equation.

760 °C along with a source temperature of 85 °C to increase the growth rate from 9 to 35 nm/h, thereby showing a scalable growth rate. Temperature-dependent resistivity measurements were performed in van der Pauw geometry (36) down to 1.8 K, as can be seen in Fig. 2C. A room-temperature resistivity (ρ) of 15 $\mu\Omega$ ·cm was obtained, slightly larger than the bulk Pt value of ~11 $\mu\Omega$ ·cm. The residual resistivity ratio (RRR), defined here as $\rho(300 \text{ K})/\rho(1.8 \text{ K})$, was 27. The resistivity versus temperature behavior was then fit with the Bloch–Grüneisen equation (37),

$$\rho = \rho_0 + \rho_{ee} T^2 + \rho_{sd} T^3 \frac{J_3(\theta/T)}{7.212} + \rho_{ss} T^5 \frac{J_5(\theta/T)}{124.14},$$
 [1]

where

$$J_N(\theta/T) = \int_0^{\theta/T} \frac{x^N dx}{(e^x - 1)(1 - e^{-x})}.$$

The Bloch–Grüneisen equation models the resistivity of metals considering contributions from electron–electron scattering ($\rho_{\rm ee}$), interband scattering ($\rho_{\rm sd}$), and intraband scattering ($\rho_{\rm ss}$) in addition to the residual resistivity (ρ_0). We found the intraband and electron–electron scattering term to be negligible. Excellent fits were obtained using only the ρ_0 and contribution from $\rho_{\rm sd}$ terms. Debye temperature $\Theta_{\rm D}$ of 232 K was determined from the fitting, agreeing well with the bulk value of 240 K (38). These observations attest to the bulk-like electronic properties and high quality of Pt thin films grown using this approach.

To show that this technique does not only apply to simple metals like Pt, thin films of the metallic binary oxide RuO2 were grown using Ru(acac)₃ with a source temperature of only 100 °C. Epitaxial and phase-pure films were obtained at the low substrate temperatures of 300 to 400 °C on TiO₂ (110) and TiO₂ (101) substrates. HRXRD patterns seen in Fig. 3 A and B show the single crystalline (110) or (101) orientation, respectively, for the RuO₂ films grown at 300 °C, with a thickness of 12 nm and 16 nm, respectively, obtained from the finite-thickness fringes. Streaky RHEED patterns (SI Appendix, Fig. S2) were seen along with atomic steps from AFM for films grown on TiO₂ (110), once again displaying the atomically smooth films this growth process allows for. Temperature-dependent resistivity measurements as shown in Fig. 3C indicate metallic behavior and resistivities approaching that of bulk RuO₂, with a lower resistivity for films grown on TiO₂ (101). The 16-nm film on TiO₂ (101) shown here had $\rho_0 = 6$ μΩ·cm and RRR = 8.

As a function of thickness, RuO₂ films grown on TiO₂ (110) revealed a decreasing resistivity with increasing thickness, a common result for thin metallic films that is likely due to finite size effects such as defects at the film/substrate interface or film's surface. As film thickness was increased beyond 18 nm, a large anisotropy occurred between the resistance along the [001] and $[1\overline{10}]$ directions, making four-terminal resistivity measurements difficult. The reason for this anisotropy is likely due to cracking of the film under tensile strain, as was observed in the previous report (10). Although both RuO₂ and TiO₂ have the rutile crystal structure, there is a large lattice mismatch of +2.3% in the $[1\overline{1}0]$ direction, causing a significant tensile strain on RuO2. Regardless, RuO₂/TiO₂ (110) showed record-low residual resistivities, comparable to recently reported e-beam MBE-grown films (10, 39), with values approaching 13 $\mu\Omega$ -cm (Fig. 3D). We do recognize, however, a small difference in the residual resistivities is likely due to the difference in the epitaxial strain.

Finally, applying the solid source MOMBE technique to more complex materials, SrRuO₃ thin films were grown on SrTiO₃ (001) substrates. At a substrate temperature of 665 °C and, again, a Ru(acac)₃ cell temperature of 100 °C, phase-pure and epitaxial films were obtained. In Fig. 3E, the HRXRD pattern of



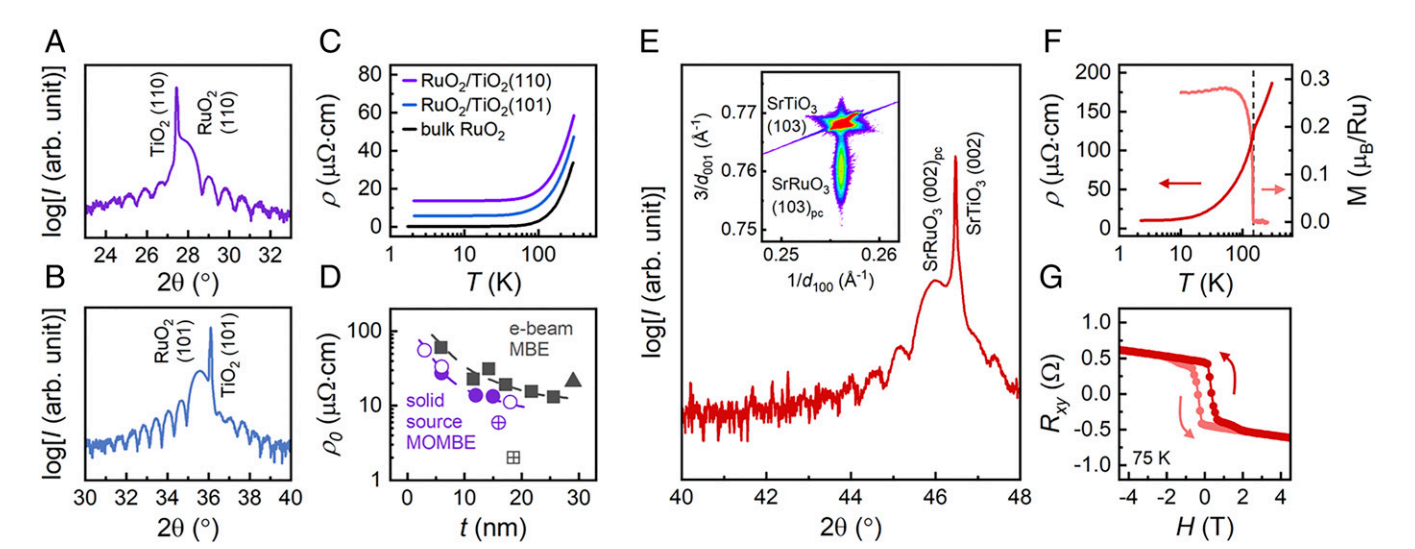


Fig. 3. HRXRD of (A) 12-nm RuO₂ film grown on TiO₂ (110) and (B) 16-nm RuO₂ film on TiO₂ (101) substrates. (C) Resistivity of A and B compared with the bulk. (D) Residual resistivity of RuO₂ films grown with two different Ru(acac)₃ precursor purities (open circles = 97% and closed circles = 99.99%) compared with recent e-beam MBE reports by Ruf et al. (10) (squares) and Uchida et al. (39) (triangle). Although it is not a direct comparison, we also include ρ_0 (for completeness) of RuO₂ films on TiO₂ (101), shown as open symbols with cross. (E) HRXRD of SrRuO₃ film grown on SrTiO₃ (001) substrate. Reciprocal space maps of (103) peak are shown in the inset. (F) Resistivity vs. temperature on the left axis and magnetization vs. temperature under zero magnetic field on the right axis for the same SrRuO₃ film. Dashed line at 149 K marks the onset of ferromagnetism. (G) Total Hall resistance at 75 K with arrows signifying the field sweep direction, forward and then reverse.

a 16-nm film can be seen with a single film peak and finitethickness fringes. Reciprocal space maps around the (103) peak showed a coherently strained film at this thickness consistent with the fully strained orthorhombic phase.

Metallic behavior was present for the entire temperature range (1.8 to 300 K) in this $SrRuO_3$ film, with a kink in the slope occurring at 149 K (Fig. 3F), around the temperature (\sim 160 K in bulk) where ferromagnetism is expected to appear (27). The onset of ferromagnetism was confirmed by a nonzero magnetic moment below 149 K (Fig. 3F) and a well-defined ferromagnetic hysteresis loop below this temperature, such as that seen in *SI Appendix*, Fig. S3 at 75 K. The saturation magnetization of \sim 0.36 μ_B/Ru achieved on cooling in a magnetic field of 2 T (*SI Appendix*, Fig. S3) along the in-plane [100] azimuth of the substrate is comparable to previously reported values from $SrRuO_3$ films (40). The ordinary and

anomalous Hall effect were also present, as expected, and can be seen in the hysteretic Hall resistance as a function of the applied magnetic field at 75 K in Fig. 3G. Comparing with SrRuO₃ films grown by PVD techniques, the RRR of 18 obtained here is larger than any reported PLD-grown (41) or sputtered films (42) but not quite as large as the highest reported MBE films (43) or bulk single crystals (44). As these films were grown with a precursor purity of only 97%, we believe there is still room for improvement with further growth optimization and by decreasing point defects with a higher purity starting material.

Discussion

The ability to synthesize atomically controlled materials continues to drive modern technology and fundamental study. Andre Geim and Kostya Novoselov were awarded the 2010 Nobel Prize in

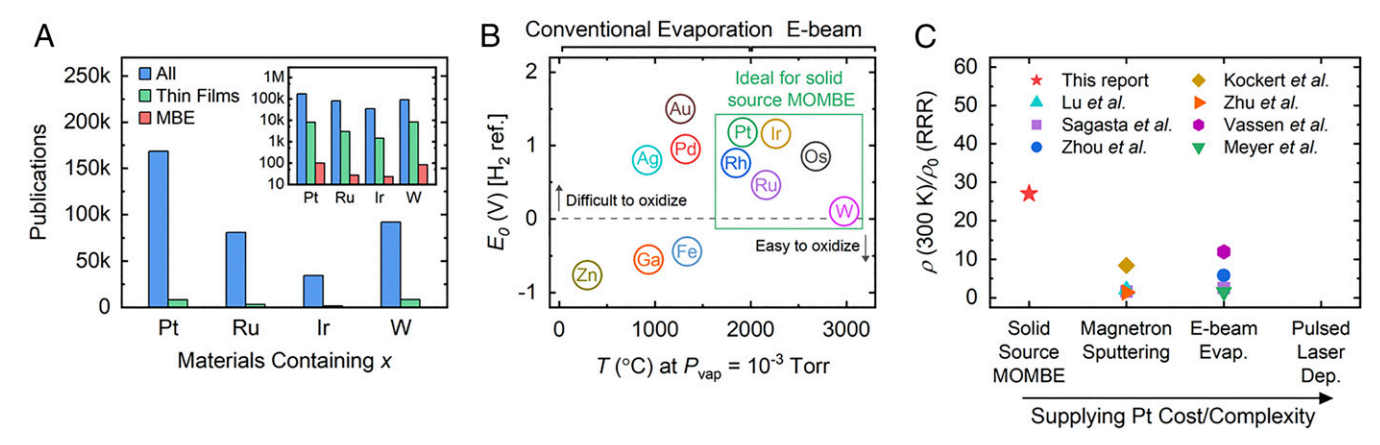


Fig. 4. (A) Number of publications (to-date) for materials containing select elements such as Pt, Ru, Ir, and W, illustrating a large gap between their importance and our ability to synthesize them in thin-film form. Blue bars represent all the publications on the topic involving materials containing Pt, Ru, Ir, and W; green bars represent the number of publications on thin films containing Pt, Ru, Ir, and W; and red bars represent the number of publications on the topic of MBE-grown films containing Pt, Ru, Ir, and W. The inset shows the same plot on the log-y scale. (B) Standard reduction potential (E_0) using an H₂ reference electrode for select metals plotted against the temperature at which their vapor pressure is 10^{-3} Torr (16). Boxed elements represent ideal candidates for solid source MOMBE due to their ultra-low vapor pressure and low oxidation potential. (C) RRR of Pt thin films from our report compared with literature reports from e-beam evaporation and magnetron sputtering PVD techniques (24, 45–50). To the best of our knowledge, there are no reports of RRR for PLD Pt films.

rise in the work involving graphene with over 200,000 publications so far. To put the potential broader impact of the solid source MOMBE approach into context, we first show in Fig. 4A the number of publications (blue bars) on different materials containing Pt, Ru, Ir, or W. A large number of publications exceeding tens of thousands highlights their relevance for both fundamental study and technological applications. In contrast, however, only a few thousand are relevant to thin films (green bars) and, even more surprisingly, only a few tens of them are on films grown using MBE. Therefore, this statistic clearly illustrates a large gap between material demand and our capability to synthesize them in an atomically controlled fashion. We recognize this difference is due to these materials containing elements with ultra-low vapor pressures. Furthermore, many of these low vapor pressure elements also possess low oxidation potential (or high reduction potential), which makes their oxidation nontrivial, especially in low-pressure PVD techniques. Fig. 4B shows standard reduction potential (E_0) of these select elements as a function of temperature at which their vapor pressure is 10^{-3} Torr (i.e., suitable for their MBE growth). Our solid source MOMBE technique therefore aims to close this publication gap by allowing for lowtemperature sublimation (at T < 100 °C) instead of the extremely high temperatures (typically 2,000 to 3,000 °C) in e-beam evaporation along with the added benefits of their preoxidized state in the metal-organic precursor. As an example of the latter, we have already shown the growth of epitaxial RuO₂ and SrRuO₃, where Ru in its preoxidized 3+ state in Ru(acac)₃ can be oxidized to the desired 4+ state using oxygen plasma, a weaker oxidant than ozone, which is typically used.

Finally, by being such a low-temperature process, the complexity and cost of supplying the metal is decreased while maintaining the quality common to MBE-grown materials. For example, keeping in mind that there are differences in substrates and thicknesses, Fig. 4C shows RRR reports for Pt films grown by PVD techniques. The solid source MOMBE-grown Pt film has the largest RRR while only requiring relatively inexpensive and simple low-temperature sublimation compared with the process of sputtering a Pt target, controlling an electron beam for evaporation, or managing a laser in PLD. We believe even larger RRR values can easily be achieved using this technique by increasing the purity of the source materials, as the ones used here were only 97% pure, and the source purity can greatly affect the residual resistivity.

Physics "for groundbreaking work regarding the two-dimensional

material graphene." It was the simplicity of exfoliation as a syn-

thesis method that made it possible for them and for a wide sci-

entific community to access this material experimentally. This

aspect of their exfoliation approach has resulted in the exponential

In summary, the solid source MOMBE approach we have developed is a unique route to supply "stubborn" metals such as Pt or Ru at operating temperatures less than 100 °C, which can be achieved in a low-temperature effusion cell as opposed to the several thousand degrees Celsius needed using e-beam evaporators. To illustrate the capability of the solid source MOMBE approach, we have demonstrated the growth of single crystalline Pt and RuO₂ films as well as the more complex SrRuO₃ films, all containing an ultra-low vapor pressure metal. Pt films with a record-high RRR value were achieved, whereas RuO₂ films revealed a record-low

residual resistivity, attesting to the ability of our approach to grow high-quality materials in an atomically controlled fashion. Likewise, SrRuO₃ films with only 97% pure Ru precursor yielded an RRR value of 18, which is already higher than those grown using PLD and sputtering approaches. We argue that the solid source MOMBE approach may potentially open up new PVD pathways (not just MBE) for "stubborn" materials such as delafossites, iridates, and tungstates containing elements that have low vapor pressures and are hard to oxidize in low-pressure PVD approaches.

Materials and Methods

An effusion cell (E-Science, Inc.) was used for the low-temperature, 65 to 85 °C, sublimation of Pt(acac)₂ (97%; MilliporeSigma) and 100 °C sublimation of ruthenium(III) acetylacetonate, Ru(acac)₃ (97% for RuO₂ and SrRuO₃; MilliporeSigma, and 99.99% for RuO2; American Elements). Sr was also supplied by an effusion cell for the growth of SrRuO₃. The powder precursors were placed directly in a pyrolytic boron nitride crucible (E-Science, Inc.) inside an effusion cell. A beam equivalent pressure of $\sim 2 \times 10^{-7}$ Torr was measured for Pt at 65 °C and $\sim 1 \times 10^{-7}$ Torr for Ru at 100 °C. Both materials were grown in an oxygen environment, as it has been shown necessary for the stabilization of the (001) epitaxial orientation (31) in Pt and to ensure complete oxidation of RuO2 and SrRuO3. Oxygen was supplied at a pressure of $5\times10^{-6}\,$ Torr by a radio frequency plasma source (Mantis) operated at 250 W and with charge deflection plates. Pt films were grown on SrTiO₃ (001) and Nb-doped SrTiO₃ (001) single-crystal substrates (Crystec GmbH). RuO₂ films were grown on TiO₂ (110) and TiO₂ (101) (MTI Corporation). SrRuO₃ films were grown on SrTiO₃ (001) (Shinkosha). Substrate temperatures were 760 °C for Pt, 300 °C for RuO₂, and 665 °C for SrRuO₃. Following growth, the films were cooled in an oxygen plasma environment. The use of oxygen plasma during growth prevented the formation of oxygen vacancies in SrTiO₃ substrate. It was confirmed by performing a controlled experiment by subjecting a bare SrTiO₃ substrate under the same thermal cycle in a vacuum showing no measurable conductivity. By placing ohmic contacts on the backside of the SrTiO₃ substrate, we further ensured the substrate remained insulated after growth.

RHEED (Staib Instruments) was carried out in situ during and after growth to monitor the film surfaces. Film surfaces after growth were also characterized using AFM (Bruker). HRXRD and reciprocal space maps were performed using a SmartLab XE X-ray diffractometer (Rigaku). Temperature-dependent four-terminal resistivity measurements were performed down to 1.8 K, using indium as an ohmic contact for Pt and aluminum for RuO2 and SrRuO3 in a DynaCool Physical Property Measurement System (PPMS, Quantum Design). Hall measurements were performed using a four-quadrant sweep of magnetic field between –9 T and +9 T normal to the film surface in the DynaCool PPMS. Temperature and magnetic field-dependent magnetization measurements were performed with a magnetic field applied along the in-plane [100] azimuth of the SrTiO3 substrate using the Vibrating Sample Magnetometer option in an EverCool Physical Property Measurement System (Quantum Design). For temperature-dependent magnetization measurements, sample was cooled under zero applied magnetic field while the data were taken upon warming.

Data Availability. All study data are included in the article and/or *SI Appendix*.

ACKNOWLEDGMENTS. We thank Fengdeng Liu for help with the MBE schematic and Darrell Schlom for helpful discussion. This work was primarily supported by the US Department of Energy (DOE) through Grant DE-SC002021. A.K.M. and T.K.T. acknowledge support from the Air Force Office of Scientific Research through Grants FA9550-19-1-0245 and FA9550-21-1-0025 and partially through NSF Grant DMR-1741801. J.Y. and A.R. acknowledge support from the US DOE through the University of Minnesota Center for Quantum Materials under Award DE-SC0016371. Parts of this work were carried out at the Characterization Facility, University of Minnesota, which receives partial support from NSF through the Materials Research Science and Engineering Centers (MRSEC) program under Award DMR-2011401.

- H. L. Stormer, Nobel lecture: The fractional quantum Hall effect. Rev. Mod. Phys. 71, 875–889 (1999).
- N. Samarth, Quantum materials discovery from a synthesis perspective. Nat. Mater. 16, 1068–1076 (2017).
- A. Gozar et al., High-temperature interface superconductivity between metallic and insulating copper oxides. Nature 455, 782–785 (2008).
- A. Ohtomo, H. Y. Hwang, A high-mobility electron gas at the LaAlO₃/SrTiO₃ heterointerface. Nature 427, 423–426 (2004).
- S. Thiel, G. Hammerl, A. Schmehl, C. W. Schneider, J. Mannhart, Tunable quasi-twodimensional electron gases in oxide heterostructures. *Science* 313, 1942–1945 (2006).
- 6. V. Umansky et al., MBE growth of ultra-low disorder 2DEG with mobility exceeding 35×10^6 cm²/V s. *J. Cryst. Growth* **311**, 1658–1661 (2009).
- J. Son et al., Epitaxial SrTiO₃ films with electron mobilities exceeding 30,000 cm² V(-1) s(-1). Nat. Mater. 9, 482–484 (2010).
- K. J. Choi et al., Enhancement of ferroelectricity in strained BaTiO₃ thin films. Science 306, 1005–1009 (2004).
- J. H. Haeni et al., Room-temperature ferroelectricity in strained SrTiO₃. Nature 430, 758–761 (2004).
- 10. J. P. Ruf et al., Strain-stabilized superconductivity. Nat. Commun. 12, 59 (2021).
- K. Ahadi et al., Enhancing superconductivity in SrTiO₃ films with strain. Sci. Adv. 5, eaaw0120 (2019).

ed at University of Minnesota Libraries on August 5, 2021

- T. Ohnishi, K. Shibuya, T. Yamamoto, M. Lippmaa, Defects and transport in complex oxide thin films. J. Appl. Phys. 103, 103703 (2008).
- J. L. MacManus-Driscoll et al., New approaches for achieving more perfect transition metal oxide thin films. APL Mater. 8, 040904 (2020).
- D. G. Schlom, Perspective: Oxide molecular-beam epitaxy rocks! APL Mater. 3, 062403 (2015).
- D. G. Schlom, L. N. Pfeiffer, Oxide electronics: Upward mobility rocks! Nat. Mater. 9, 881–883 (2010).
- F. Macdonald, D. R. Lide, CRC handbook of chemistry and physics: From paper to web. Abstr. Pap. Am. Chem. Soc. 225, U552 (2003).
- W. Braun, J. Mannhart, Film deposition by thermal laser evaporation. AIP Adv. 9, 085310 (2019).
- S. A. Chambers, Epitaxial growth and properties of thin film oxides. Surf. Sci. Rep. 39, 105 (2000).
- B. Jalan, R. Engel-Herbert, N. J. Wright, S. Stemmer, Growth of high-quality SrTiO₃ films using a hybrid molecular beam epitaxy approach. *J. Vac. Sci. Technol. A* 27, 461–464 (2009).
- 20. A. Prakash et al., Hybrid molecular beam epitaxy for the growth of stoichiometric BaSnO₃. J. Vac. Sci. Technol. A 33, 060608 (2015).
- J. A. Moyer, C. Eaton, R. Engel-Herbert, Highly conductive SrVO₃ as a bottom electrode for functional perovskite oxides. Adv. Mater. 25, 3578–3582 (2013).
- R. Hiskes et al., Single source metalorganic chemical vapor-deposition of low microwave surface-resistance YBa₂Cu₃O₇. Appl. Phys. Lett. 59, 606–607 (1991).
- Z. Lu et al., Solid source MOCVD for the epitaxial-growth of thin oxide-films. J. Cryst. Growth 128, 788–792 (1993).
- 24. E. Sagasta et al., Tuning the spin Hall effect of Pt from the moderately dirty to the superclean regime. Phys. Rev. B 94, 060412 (2016).
- C. C. Hu, K. H. Chang, M. C. Lin, Y. T. Wu, Design and tailoring of the nanotubular arrayed architecture of hydrous RuO₂ for next generation supercapacitors. *Nano Lett.* 6, 2690–2695 (2006).
- J. Rossmeisl, Z. W. Qu, H. Zhu, G. J. Kroes, J. K. Norskov, Electrolysis of water on oxide surfaces. J. Electroanal. Chem. (Lausanne) 607, 83–89 (2007).
- G. Koster et al., Structure, physical properties, and applications of SrRuO₃ thin films. Rev. Mod. Phys. 84, 253–298 (2012).
- N. B. Morozova et al., Vapor pressure of precursors for CVD on the base of platinum group metals. J. Phys. IV 11, 609–616 (2001).
- S. Flanagan et al., A design-of-experiments approach to modeling activity coefficients in solvent mixtures: A case study using platinum(II) acetylacetonate in mixtures of acetone, cyclohexanol, 1,2,3,4-tetrahydronaphthalene and propylene carbonate. Green Chem. 7, 333–338 (2005).
- 30. W. Wang, L. Zhang, Hydrogen transfer hydrogenation of nitrobenzene to aniline with Ru(acac)₃ as the catalyst. Res. Chem. Intermed. 40, 3109–3118 (2014).

- M. Hecq, A. Hecq, Oxygen induced preferred orientation of dc sputtered platinum. J. Vac. Sci. Technol. 18, 219–222 (1981).
- A. Kahsay et al., Growth of epitaxial Pt thin films on (001) SrTiO₃ by rf magnetron sputtering. Appl. Surf. Sci. 306, 23–26 (2014).
- J. Son, J. Cagnon, S. Stemmer, Strain relaxation in epitaxial Pt films on (001) SrTiO₃
 J. Appl. Phys. 106, 043525 (2009).
- M. Kasai, H. Dohi, Surface structure and electrochemical properties of platinum films grown on SrTiO₃(100) substrates. Surf. Sci. 666, 14–22 (2017).
- H. Galinski et al., Agglomeration of Pt thin films on dielectric substrates. Phys. Rev. B Condens. Matter Mater. Phys. 82, 235415 (2010).
- L. J. van der Pauw, A method of measuring the resistivity and Hall coefficient on lamellae of arbitrary shape. *Philips Techn. Rev.* 20, 220–224 (1958).
- D. B. Poker, C. E. Klabunde, Temperature-dependence of electrical-resistivity of vanadium, platinum, and copper. *Phys. Rev. B Condens. Matter* 26, 7012–7014 (1982).
- 38. W. T. Berg, Low temperature heat capacity of platinum. J. Phys. Chem. Solids 30, 69–72 (1969).
- M. Uchida, T. Nomoto, M. Musashi, R. Arita, M. Kawasaki, Superconductivity in uniquely strained RuO₋₂ films. *Phys. Rev. Lett.* 125, 147001 (2020).
- R. Gao et al., Interfacial octahedral rotation mismatch control of the symmetry and properties of SrRuO₃. ACS Appl. Mater. Interfaces 8, 14871–14878 (2016).
- F. Chu et al., Microstructures and electrical properties of SrRuO₃ thin films on LaAlO₃ substrates. J. Electron. Mater. 25, 1754–1759 (1996).
- Q. Gan, R. Rao, C. Eom, J. Garrett, M. Lee, Direct measurement of strain effects on magnetic and electrical properties of epitaxial SrRuO₃ thin films. *Appl. Phys. Lett.* 72, 978–980 (1998).
- H. P. Nair et al., Synthesis science of SrRuO₃ and CaRuO₃ epitaxial films with high residual resistivity ratios. APL Mater. 6, 046101 (2018).
- N. Kikugawa et al., Single-crystal growth of a perovskite ruthenate SrRuO₃ by the floating-zone method. Cryst. Growth Des. 15, 5573–5577 (2015).
- S. Meyer et al., Temperature dependent spin transport properties of platinum inferred from spin Hall magnetoresistance measurements. Appl. Phys. Lett. 104, 242411 (2014).
- R. Vassen, P. Jung, Interstitial migration of hydrogen and helium in platinum. Phys. Rev. B Condens. Matter 37, 2911–2917 (1988).
- 47. L. Zhu, L. Zhu, M. Sui, D. C. Ralph, R. A. Buhrman, Variation of the giant intrinsic spin Hall conductivity of Pt with carrier lifetime. *Sci. Adv.* 5, eaav8025 (2019).
- M. Kockert, R. Mitdank, A. Zykov, S. Kowarik, S. F. Fischer, Absolute Seebeck coefficient of thin platinum films. J. Appl. Phys. 126, 105106 (2019).
- Y. M. Lu et al., Pt magnetic polarization on Y₃Fe₅O₁₂ and magnetotransport characteristics. Phys. Rev. Lett. 110, 147207 (2013).
- H. Zhou, P. Wochner, A. Schops, T. Wagner, Investigation of platinum films grown on sapphire (0001) by molecular beam epitaxy. J. Cryst. Growth 234, 561–568 (2002).